J Mater Sci (2007) 42:6798–6802
DOI 10.1007/s10853-006-1402-z

Mechanical properties and microstructure of Al_2O_3/mullite composite

F. C. Zhang · H. H. Luo · S. G. Roberts

Received: 3 November 2006 / Accepted: 4 December 2006 / Published online: 26 April 2007

Abstract An Al_2O_3/5 vol.% mullite composite was synthesized by using reaction sintering of Al_2O_3/0.78 wt.% SiC at 1,600 °C for 2 h in air. The phase analysis of the Al_2O_3/mullite composite was carried out using X-ray diffraction (XRD). There were two kinds of mullite in alumina/mullite composite, namely, $3Al_2O_3{\cdot}2SiO_2$ and $Al_{5.65}Si_{0.35}O_{9.175.}$ The microstructure of the Al_2O_3/mullite composite was investigated using scanning electron microscope (SEM) and transmission electron microscope (TEM). The mechanical properties such as Young's modulus, Poisson's ratio, hardness, toughness and strength of the Al_2O_3/mullite composite were investigated. The influence of mullite on the composite is discussed.

Introduction

Mullite is a characteristic constituent of all ceramic products made from aluminosilicates, and has recently become a candidate as a high-temperature structural ceramic [1–4], because of its excellent physical properties, such as low dielectric constant, low thermal expansion, high melting point, high resistance to creep, high temperature mechanical stability and thus high thermal shock resistance, and chemical corrosion [5].

An Al_2O_3–SiC nanocomposite is a thermodynamically metastable system at elevated temperatures in air or in the presence of oxygen [6]. Similar to the conventional SiC ceramics and SiC whisker-reinforced ceramic composites, SiC particles in the nanocomposite, especially those near to the sample surface, are susceptible to oxidation at temperatures above 1,000 °C,forming silica, which may subsequently react with the Al_2O_3 matrix. Therefore, a reacted surface scale is expected to form in the Al_2O_3/SiC nanocomposites when subjected to oxidation in air at high temperatures. Furthermore, microstructural change, such as at grain boundaries, may occur in the bulk region of the aged nanocomposites although oxidation may not take place in this region. Sakka et al. described a new method for processing SiC–mullite–Al_2O_3 nanocomposites by the reaction sintering of green compacts prepared by colloidal consolidation of a mixture of SiC and Al_2O_3 powders [7]. In this method, the surface of the SiC particles was first oxidized to produce silicon oxide. This reduced the core of the SiC particles to nanometer size. Next, the surface silicon oxide was reacted with alumina to produce mullite. This process resulted in particles with two kinds of morphologies: nanometer-sized SiC particles that were distributed in the mullite phase and mullite whiskers in the SiC phase. Both particle types were immersed in the Al_2O_3 matrix.

Wang et al. [8, 9] investigated the reaction in Al_2O_3/5 vol.% SiC composite in air for various periods at 1,400 °C. The thermal treatment lead to the SiC particles within the surface scale being oxidized to form silica, which subsequently reacted with the Al_2O_3 matrix and transformed to mullite. The reaction thickness increased

F. C. Zhang · H. H. Luo (✉)
State Key Laboratory of Metastable Materials Science and Technology, Yanshan University, Qinhuangdao 066004, P.R. China
e-mail: haihui_luo@126.com

F. C. Zhang
e-mail: zfc@ysu.edu.cn

S. G. Roberts
Department of Materials, University of Oxford, Oxford OX1 3PH, UK

with the increasing of the aging time at the aging temperature. The surface scale exhibited a porous microstructure, consisting of alumina grains, mullites of differing composition, and amorphous silica and silicate pockets. Two types of mullite phase, which contain a high and a low level of silica, have been identified in the surface scale.

The aim of the present work was to investigate the response of microstructure and mechanical properties for an Al_2O_3/SiC nanocomposite sintered at 1,600 °C in air.

Experimental

Material and specimen preparation

The nanocomposite powders used in this study were the mix powders of Al_2O_3 with 0.78 vol.% SiC. The silicon carbide powder and alumina powder were commercial α-SiC powder with an average particle size of 200 nm (UF25, Lonza, Germany) and α-Al_2O_3 powder with a 400 nm average particle size (AES11C, Sumitomo Chemicals, Tokyo, Japan).

During the specimen preparation, the SiC powder was dispersed in 50 ml of distilled water together with 10 drops of dispersing agent (Dispex A40, Allied Colloids, UK) and 4% PEG. The SiC powder was then added to Al_2O_3 powder and attrition milled at 500 rpm for 2 h. The resultant slurry was freeze-dried for 24 h in vacuum, and the dried powder was passed through a 150-μm sieve. Green bodies were prepared from the sieved powder by uniaxial pressing in a 30 mm die with an applied pressure of about 90 MPa. The thickness of the green body was 5 mm. The same treatment was also applied to Al_2O_3 powders without SiC content.

A Carbolite Furnace (Bamford, Sheffield S 30 2 AU, England) was employed to sinter the samples. The sintering procedure was such that the compacts were sintered in a bed of Al_2O_3 beads in air at 1,600 °C for 2 h under heating rate and cooling rate at 4 °C/min.

Experimental procedure

The Archimedes method was introduced in this paper to measure the density of the samples sintered by using water as an immersion medium. The relative density was calculated using the theoretical densities of alumina (3.96 g cm^{-3}), silicon carbide (3.05 g cm^{-3}) and mullite (3.19 g cm^{-3}). The theoretical density of the Al_2O_3/5 vol.% mullite is 3.91 g cm^{-3} according to the reacting formula of alumina and silicon carbide.

Phase compositions were identified by X-ray diffraction (XRD) analysis with CuK_α radiation through a Phillips Model θ-2θ Diffractometer. A Philips PW1729 generator and detector APD system were used to collect data. Both of the center and surface of the sample were used to analyze the phase composition. External standard method was used for quantitative phase analysis.

The polishing test was carried out to prepare SEM samples by an automatic polishing machine (Model Motopol 2000 Grinder/Polisher, Buehler UK Ltd, Coventry England) using Kenet plates with 25 μm, 6 μm, 3 μm and 1 μm grits (Engis Ltd., UK) and liquid diamond (Kemet International Ltd, UK). The polishing plate, rotating at about 60 rpm and an external load of 15 N were used on the specimens. The 6 μm and 3 μm grit polishing steps were carried out on hard cloths; a soft cloth was used for the final 1 μm polishing. After polishing, the samples were thermally etched at 1,450 °C for 1 h in a vacuum furnace (Lenton, UK), then the SEM specimen was coated with a gold layer using a SEM Coating System (Gold Coater). The eroded surface of the composite was investigated by using a Hitachi Model S520 SEM. The average grain size of each specimen was measured using a standard line from SEM micrographs of thermal etched polished surface, counting at least 300 intercepts for each micrograph. A Hitachi model TEM H-800 was employed to investigate the microstructure of the sample. The TEM specimens were prepared following standard grinding and ion-polishing procedures.

Young's modulus (E) and Poisson's ratio (v) were measured by a resonance method using a Grindosonic machine (Model MK 5, J. W. Lemmens, Leuven, Belgium). The sample size was $2 \times 3 \times 20$ mm.

The flexural strength data was obtained through four-point bend tests. Rectangular bar samples of size ~$22 \times 3 \times 1.5$ mm were used for all tests. Samples were cut along the long dimension parallel to the grinding direction. Both of the tensile and compressive faces and the other two sides of each sample were machined and then fully polished. The polishing process was carried out using an automatic polishing machine (Model Motopol 2000 Grinder/Polisher, Buehler UK Ltd, Coventry England). The first two polishing steps each removed at least 200 μm of materials with diamond grits of 25 μm and 6 μm grit size. The third and fourth steps each removed about 50 μm using 3 μm and 1 μm diamond. This procedure was used in order to remove the influence of surface grinding and results in a surface whose properties were determined by the final polishing steps. All four-point bend tests were carried out in a DMG model machine (Rubicon Co. England) with a 3 kN load cell head at a cross-head displacement speed of 0.1 mm/min using a four-point bending rig with an inner span of 9 mm and an outer span of 20 mm. The mean strength and standard deviation for each of the conditions studied was obtained using six specimens. XY plot software was used for the collection of the experimental data.

Fracture toughness of the sample was measured by indentation methods using a Hardness Tester. The fracture toughness (K_{IC}) of the sample was calculated by Anstis, Chantikul, Lawn and Marshall equation (1981), i.e., $K_{IC} = 0.016(E/H)^{1/2}(P/c^{3/2})$, where E is the Young's modulus of the sample. $H = 1{,}854.4P/(2a)^2$, where P is the indenter load, a is the indentation half-diagonal length, c is surface radial crack length [10]. The indenter loads selected for this study were 1, 2, 5 and 10 kg. Hardness of the sample was measured by indentation methods using a Hardness Tester. The indentation load was 2 kg.

Results and discussion

Figure 1 shows the XRD diagram of samples. Clearly, there were four kinds of phases in the Al_2O_3/0.78 wt.% SiC nanocomposite sintered at 1,600 °C, they were alumina (α-Al_2O_3), standard mullite ($3Al_2O_3{\cdot}2SiO_2$), less silicon and oxygen mullite ($Al_{5.65}Si_{0.35}O_{9.175}$) and zirconium oxide ($ZrO_2$). Both the XRD patterns of center and surface of the Al_2O_3/0.78 wt.% SiC nanocomposite sintered at 1,600 °C were the same. Quantitative phase analysis indicated that the mullite content in Al_2O_3/mullite composite was 5 vol.% and there was about 1 vol.% ZrO_2 in both samples. In order to check where the zirconium oxide came from in the samples, a sample of pure alumina non-milled and sintered at 1,600 °C was analyzed using XRD. The result indicated that there was no ZrO_2 in the sample, so the ZrO_2 must come from milling ball.

Table 1 lists the basic properties of samples investigated in this paper and the Al_2O_3/5 vol.% SiC in other work [11]. The relative density of the Al_2O_3 and the Al_2O_3/5 vol.% mullite samples were 98.2% and 97.9%, respectively, which indicated that samples with very high density could be obtained after sintering at 1,600 °C.

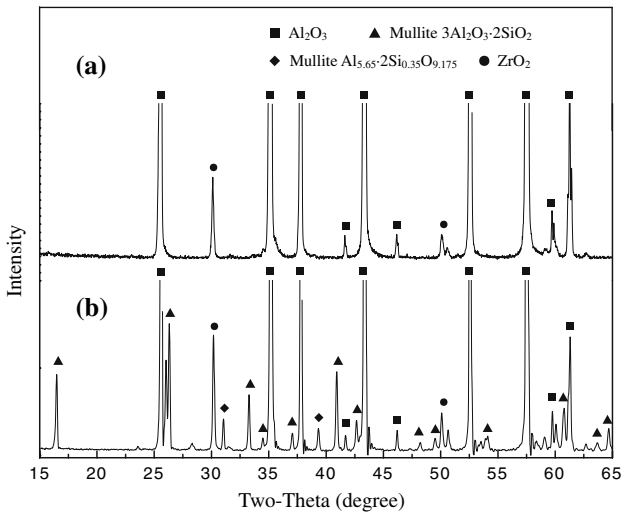

Fig. 1 XRD diagram of samples without (**a**) and with (**b**) 5 vol.% mullite content

Figure 2 gives the microstructures of samples without and with 5 vol.% mullite content. For all samples, several light color particles appear in some area of the micrographs, which are ZrO_2 from the wear of milling media and the attritor bucket during milling, the XRD results above can prove it. The grain size of Al_2O_3/5 vol.% mullite composite was finer than that of Al_2O_3 sample (Table 1), indicating that mullite could retard the grain growth of matrix in sintering.

Mechanical properties were summarized in Table 1. The Young's modulus and Poisson's ratio for all samples were almost the same. The strength of samples with and without mullite content were 494 MPa and 409 MPa, respectively. The fracture toughness were 3.30 MPa $m^{1/2}$ for Al_2O_3 and 2.98 MPa $m^{1/2}$ for Al_2O_3/5 vol% mullite. The hardness of samples with and without mullite content were 16.9 GPa and 16.2 GPa, respectively. It was indicated that the mullite strengthened the composite but deteriorated its fracture toughness, and have little influence on hardness. As far as mechanical properties were concerned, the particle-reinforced composite investigated in this paper is superior to laminated alumina/mullite composite [12], but inferior to alumina/mullite whisker composite [13].

Figure 3 gives the TEM analysis results of the Al_2O_3 and Al_2O_3/5 vol.% mullite composite. Iconograph in Fig. 3b is diffraction spot of mullite. It was indicated that the mullite in the sample (black and white particles in Fig. 3b) was spheral with size from about 100 to 700 nm (with mean size of about 400 nm) in diameter and embedded in the alumina grain or on the grain boundary. However, the mullite on the alumina grain boundary was much more than that in the alumina grain, so the mullite can retard the growth of the alumina grain resulting in a finer grain size (Table 1). Lots of mullite particles (white particles in Fig. 3b) were off the matrix during preparing the TEM sample, which indicated that the strength between the mullite and the matrix was very low, so the alumina/5 vol.% mullite composite exhibited relative low mechanical properties compared with the well-investigated alumina/5 vol.% SiC nanocomposite [11].

Because the thermal expansion coefficients of Al_2O_3 and mullite are different ($8.6–9.5 \times 10^{-6}$/K and $4.5–5.7 \times 10^{-6}$/K, respectively), there are residual stress in samples induced by shrinkage dismatch of the phases. The residual stress state is such that the mullite particles are in approximately hydrostatic compression, and there are tensile hoop stresses in the surrounding matrix [14]. The hoop stresses around the intragranular particle may be sufficient to attract an intergranular crack out of the grain boundary and into the bulk of grain. Once the crack tip has

Table 1 Summary of properties of materials investigated

Material	ρ (%)	Grain size (μm)	σ_f (MPa)	K_{IC} (MPa $m^{1/2}$)	Hv (GPa)	E (GPa)	v
Al_2O_3	98.2	2.4 ± 0.51	409 ± 34	3.30 ± 0.27	16.2 ± 0.5	350 ± 2	0.23
Al_2O_3/5 vol.% mullite	97.9	2.2 ± 0.36	494 ± 25	2.98 ± 0.21	16.9 ± 0.5	343 ± 3	0.23
Al_2O_3/5 vol.% SiC [11]	99.8	4.0 ± 1.1	646 ± 41	4.6 ± 0.1	–	–	–

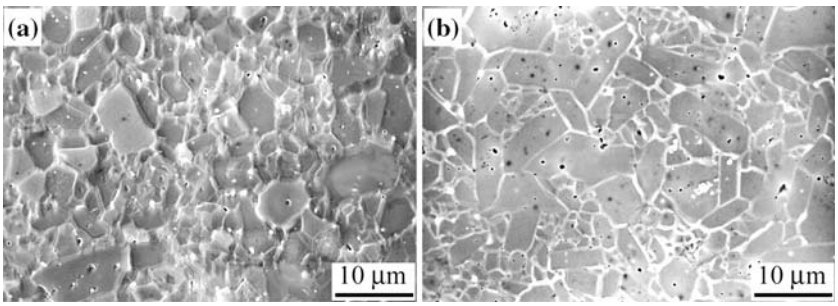

Fig. 2 Microstructures of samples without (**a**) and with (**b**) 5 vol.% mullite content

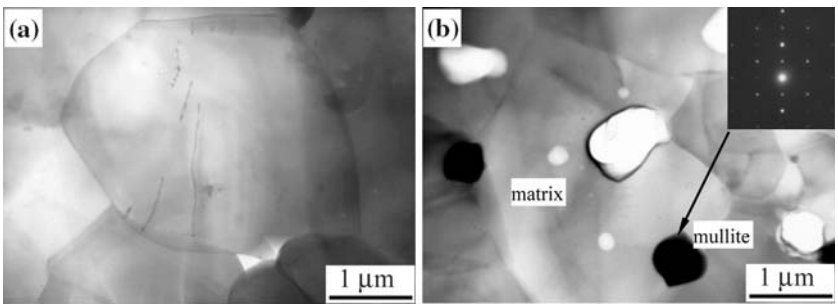

Fig. 3 TEM micrographs of samples without (**a**) and with (**b**) 5 vol.% mullite content

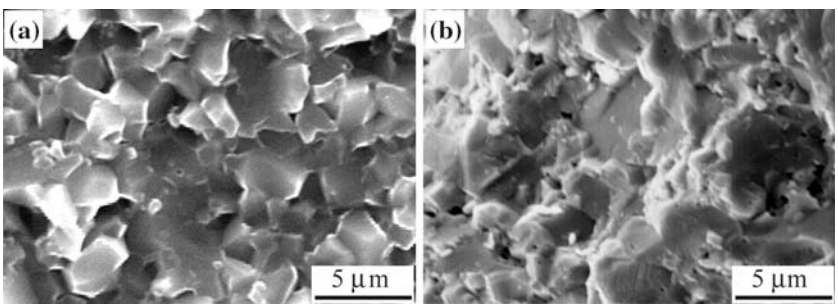

Fig. 4 Fracture surfaces of samples without (**a**) and with (**b**) 5 vol.% mullite content

propagated along its new transgranular path beyond the tensile hoop stresses of the mullite particle, it experiences the high strength of the grain interior, so the composite exhibited higher flexural strength than Al_2O_3 (Table 1). However, the fracture toughness of Al_2O_3/5 vol.% mullite composite was lower than that of Al_2O_3, the reason is still unclear, fracture mode transition showed in Fig. 4 may play a leading role in it [15].

Conclusions

1. Alumina/mullite composite was synthesized by using reaction sintering of alumina/silicon carbide in air. There were two kinds of mullite in the sintered sample, i.e., $3Al_2O_3{\cdot}2SiO_2$ and $Al_{5.65}Si_{0.35}O_{9.175}$.
2. The alumina/mullite composite exhibited average mechanical properties, with flexural strength of 494 MPa and fracture toughness of 2.98 MPa $m^{1/2}$.
3. The mullite in the sample was spheral with mean size of about 400 nm in diameter and embedded in the alumina grain or on the alumina grain boundary.

Acknowledgements The authors wish to thank Dr. Richard Todd for his helpful discussions, and his invaluable expertise in this field was greatly appreciated. The work is supported by Personnel Department of Hebei Province.

References

1. Takei T, Kameshima Y, Yasumori A, Okada K. (1999) J Am Ceram Soc 82:2876
2. Chen CY, Lan GS, Tuan WH (2000) J Eur Ceram Soc 20:2519
3. Ibrahim DM, Naga SM, Kader ZA, Salam EA (1995) Ceram Int 21:265
4. Taktak S, Baspiar MS (2005) Mater Design 26:459
5. Sato T, Shizuka M, Shimada M (1986) Ceram Int 12:61
6. Luthra KL (1988) J Am Ceram Soc 71:274
7. Sakka Y, Bidinger DD, Aksay IA (1995) J Am Ceram Soc 78:479
8. Wang J, Ponton CB, Marquis PM (1996) Scr Mater 34:935
9. Wang J, Ponton CB, Marquis PM (1995) J Mater Sci 30:321, DOI: 10:1007/BF00354391
10. Ponton CB, Rawlings RD (1989) Mater Sci Technol 5:865
11. Anya CC (1999) J Mater Sci 34:5557, DOI: 10:1023/A:1004729015686
12. Katsuki H, Ichinose H, Shiraishi A, Takaqi H, Hirata Y (1993) J Ceram Soc Jpn 9:1041
13. Tamari N, Kondoh I, Tanaka T, Katsuki H (1993) J Ceram Soc Jpn 6:704
14. Root JH, Sullivan JD, Marple BR (1991) J Am Ceram Soc 74:579
15. Kim BN, Kishi T (1994) Mater Sci Eng A 176:371